This work was carried out in whole or in part within the framework of the NOMATEN Center of Excellence, supported from the European Union Horizon 2020 research and innovation programme (Grant Agreement No. 857470) and from the European Regional Development Fund via the Foundation for Polish Science International Research Agenda PLUS programme (Grant No. MAB PLUS/2018/8).

This is the accepted manuscript submitted to:  Phys. Status Solidi B 2023, 2200567, 2 March 2023 with the embargo period till: 2 March 2024.

DOI: 10.1002/pssb.202200567

# Dynamical pathways for the interaction of $O_2$, $H_2O$, $CH_4$, and $CO_2$ with $\alpha$-alumina surfaces: Density functional tight–binding calculations

F. J. Dominguez-Gutierrez,[1, 2] Amil Aligayev,[1, 3] Wenyi Huo,[1, 3]
Muralidhar Chourashiya,[1, 4, 5] Qinqin Xu,[1] and and Stefanos Papanikolaou[1]

[1]*NOMATEN Centre of Excellence, National Center for Nuclear Research, 05-400 Swierk/Otwock, Poland*
[2]*Institute for Advanced Computational Science, Stony Brook University, Stony Brook, NY 11749, USA*
[3]*College of Mechanical and Electrical Engineering,*
*Nanjing Forestry University, Nanjing, 210037, China*
[4]*Technion, Israel Institute of Technology, Haifa, 32000, Israel*
[5]*Guangdong Technion Israel Institute of Technology, Shantou, 515063, China*

In this study, we investigated the physisorption mechanisms of $O_2$, $H_2O$, $CH_4$, and $CO_2$ molecules on alumina and their effect on electronic properties. We employed quantum-classical molecular dynamics simulations and the self-consistent-charge density-functional tight-binding (SCC-DFTB) approach to dynamically model these mechanisms. Our results revealed the binding pathways of O, H, and C atoms in the various molecules to Al and O atoms at the top atomic layers of the $\alpha-$alumina surface. We examined several adsorption sites and molecular orientations relative to Al-terminated and Ox-terminated alumina surfaces and found that the most stable physisorbed state on the Al-terminated surface is located above the Al atom, while the Ox-terminated state is found above the oxygen, resulting in enhanced optical adsorbance. The dissociation of $CH_4$ into $CH_2$+$H_2$ after interaction with the surface resulted in hydrogen production, but with low adsorbate rates. While, $O_2$ molecules primarily bond to the Al atoms, leading to the highest adsorbance rate among the other molecules. Our findings provide important insights into the physisorption mechanisms of molecules on alumina and their impact on electronic properties.

## I. INTRODUCTION

$\alpha$-Alumina, i.e., corundum, is one of the most widely used ceramic materials due to its excellent properties, such as high chemical stability, high thermal resistance, and high electrical resistance, and is considered to be an excellent adsorbent, with primary examples being radiation, high temperature and corrosion[1–6]. The interface reactions of oxide/molecules dominate in many fields, such as lubricants[7,8], electronic industries[9], automobile engines[10,11] and other transportation systems[12,13]. This material is utilized as an adsorbent, catalyst, and catalyst support in several environmentally environmentally important. . Ferri *et al.* studied CO adsorption on catalytic solid/liquid interfaces by performing ATR-IR spectroscopy[14]. Mason *et al.* reported the adsorption energy of Pb(II) onto the {0001} surface of $\alpha$-$Al_2O_3$ and $\alpha$-$Fe_2O_3$ based on DFT calculations[15]. Moreover, alumina is also used as a desiccant, which is a substance that absorbs moisture, and in water treatment as a filter medium. Experimental exploration of aluminum–assisted water split reactions has shown that the formation of an alumina film inhibits the direct reaction of Al with $H_2O$. However, when Al is alloyed with other metals (such as gallium, etc.) or prepared aluminum–based composites by ball milling modify the Al–water system for hydrogen production. Such technology for onboard hydrogen production is of great interest in a hydrogen economy[16]. Finally, optical adsorption on alumina surfaces is a process where light is absorbed resulting in to a reduction in the light intensity as it passes through. This absorption provides useful information about the electronic and optical properties of the alumina surface, including its bandgap, surface state, and surface morphology where different molecules can affect these properties[17–19].

Atomistic simulations are now used as a guide for experimental adsorption measurements, which are complicated to carry out for alumina materials due to the complex crystal structure and surface defects. For this reason, atomistic simulations are important in the investigation of physisorption processes, making advantages in understanding the underlying physical and chemical mechanisms, where alumina surfaces can be manipulated by the adsorption of different molecules such as $H_2O$, $O_2$, CO, and $CH_4$[20–22]. Although computations by the density functional density (DFT) method can provide accurate results, for large systems with open boundaries the computational demands may become prohibitively expensive and may require the use of specialized high-performance computing resources[23]. Additionally, as the number of atom types in a system increases, the number of electrons also increases, and the approximations made in DFT calculations may become even more computationally expensive.

In several cases, computationally economical simulations based on empirical or fitted interatomic potentials, such as the ReaxFF method[24] can be applied to compute the mechanical properties of alumina surfaces in good agreement with experimental data[25]. ReaxFF is based on a bond order formalism to enable the description of the bond breaking processes; however, charge transfer processes due to oxygen vacancy migration require a semi–classical approximation for modeling chemical bonding[26] in more fundamental processes. Besides, the electronic structure of the system needs explicit information[27,28] for electron–electron interactions, most notably density functional theory (DFT), as a standard software in computational materials science with high computational resource demands.

The previous discussion motivates us to utilize the self–consistent–charge density–functional tight–binding (SCC–DFTB) approach[29–31], which requires minimal computational resources through DFT packages and provides a connection between classical approaches and electronic structure theory. This approach uses a minimal set of electronic states of the surface that are represented by a set of linear equations describing the interactions between the localized orbitals. These equations take the form of a Kohn–Sham Hamiltonian matrix, which is then solved to obtain the electronic eigenstates and eigenvalues of the system. This method is currently a versatile tool for investigations in chemistry and materials science[32] due to the possibility of calculations of large systems and performing simulations for longer time scales than DFT for extensive studies on dynamical properties in DFTB. This method has several features that are helpful to understand the mechanisms of the molecular adsorption process on alumina surfaces, giving us the opportunity to model the dissociation and formation of molecules due to the interactions of X-atoms with Al and O atoms at the top layer of the surface. This type of modeling can be very expensive computationally for DFT software requiring long wall times and HPC resources.

In this work, we investigate the interaction at interfaces of $\alpha$–$Al_2O_3$ with several molecules based on systematic calculations by DFTB, followed by performing quantum-classical molecular dynamics simulations of molecular adsorption at room temperature. This work will help understand the surface interaction of alumina with water, oxygen, carbon monoxide, and methane that is essential to design, optimize, and control their applications in hydrogen production as well as a variety of sensor designs. The manuscript is organized as follows: In Section II, we describe the computational methodology for carrying out binding energy calculations by considering different physisorption pathways, optical adsorption, and dynamic mechanism of molecular adsorption. In Section III, we present the results for the calculated equilibrium molecule surface distance, adsorption rates, and adsorbance with the corresponding effect on the density of defects of the alumina surface. Finally, in Section IV, concluding remarks are summarized.

## II. METHODS

The SCC-DFTB method is an approximation to traditional Density Functional Theory (DFT) that takes into account valence electron interactions during dynamics. It involves solving Kohn–Sham equations to obtain total valence electronic densities and energies for each atom using a Hamiltonian functional based on a two-center approximation and optimized pseudo–atomic orbitals as basis functions. Slater–Koster parameter files containing tabulated Hamiltonian matrix elements, overlap integrals[29], and repulsive splines fitted to DFT dissociation curves are read into the computer memory only once at the start of the simulation[33]. Thus, the total energy of the system is expressed as

$$E^{\mathrm{DFTB}} = E_{\mathrm{band}} + E_{\mathrm{rep}} + E_{\mathrm{SCC}}, \tag{1}$$

with the band structure energy, $E_{\mathrm{band}}$, defined from the summation of the orbital energies $\epsilon_i$ over all occupied orbitals $\Psi_i$; the repulsive energy $E_{\mathrm{rep}}$ for the core–core interactions related to the exchange–correlation energy and other contributions in the form of a set of distance–dependent pairwise terms; and an SCC contribution, $E_{\mathrm{SCC}}$, as the contributions given by charge–charge interactions in the system.

In this study, we utilize the SKF pair potentials set for materials science simulations (MATSCI) that have been applied to study chemical reactions on gibbsite surfaces[34], monodentate, bidentate and tridentate adsorption of the acids on all possible adsorption sites on the alpha–alumina surfaces considering different surface coverages[35], and stability, electronic, and mechanical properties of imogolite nanotubes[36]. The electronic energies are calculated as a sum over the occupied KS single-particle energies and the sum over diatomic repulsive energy contributions. SCC corrections, as implemented in the DFTB+ code ver. 22.2[29], are included in the total energy via an iteration procedure that converges to a new electron density at every time step during the simulation, where the convergence is improved by using an electronic temperature of 1000 K.

### A. Binding energies

Corundum ($\alpha$–alumina) has a trigonal structure with oxygen ions arranged in a hexagonal close packing (HCP). Al atoms occupy two–thirds of the octahedral vacancies in the oxygen sublattice at alternating positions above and below the center of these sites. The unit cell for alumina is defined at the basal crystal orientation {0001}, which is a crystal plane perpendicular to the crystal's axis of symmetry and lying in its base. With 60 atoms - 24 Al and 36 O - the cell has hexagonal symmetry with parameters $a = 0.472$ nm, $c = 1.299$ nm, $\alpha = \beta = 90^o$, and $\gamma = 120^o$. The Al–O bond lengths, 0.0185 nm and 0.0194 nm, were optimized using DFTB+ with the conjugate gradient method (Fig. 1.) and are in good agreement with experimental data[35] ($a = 0.4763$ nm, $c = 1.3$ nm). In addition, the geometries of the isolated $O_2$, $H_2O$, $CH_4$, and $CO_2$ are optimized with an energy convergence tolerance of $10^{-6}$ eV.

The total energies, $E(z)$, of the molecule–alumina system with a separation $z$ between the top atomic layer and the center of mass of the molecule are varied above the surface in a range of 0.5 to 7 Å, which defines the computation of the adsorption potential as a function of the distance separation. The total energy is then computed as:

$$E(z) = E_{\text{Tot}} - \left(E_{\text{Surface}} + E_{\text{Molecule}}\right), \tag{2}$$

where $E_{\text{Surface}}$ is the total energy of the alumina surface; $E_{\text{Molecule}}$ is the total energy of the isolated molecule: $O_2$, $H_2O$, $CH_4$, and $CO_2$; and $E_{\text{Tot}}$ is the energy of the interacting system at every $z$–distance. Thus, the binding energy is defined as $E_b = E(z_{\text{min}})$ with $z_{\text{min}}$ as the equilibrium molecule–surface distance. Total energy calculations are performed for the molecule–alumina system, varying the distance between the surface and the center of mass of the molecules along the $z$–axis. We consider 8 different adsorption sites based on the hexagonal arrangement of aluminum atoms on the Al–terminated surface and the BCC configurations of oxygen atoms on the Ox-terminated surface. The molecular symmetry plane determines the perpendicular and parallel orientations with respect to the surface plane in the calculations. The repulsive potential is cut off at a distance below the second nearest-neighbor interaction region for numerical stability. However, this approximation may not always provide satisfactory dissociation curves. The SCC-DFTB framework addresses this limitation by shifting the repulsive energy functions downward.

### B. Optical absorption spectra

The optical absorption is investigated within the DFTB framework as an electronic dynamic process in response to an external electric field[37,38]. The conventional adiabatic approximation gives the time evolution of the electron density matrix by time integration of the Liouville-von Newmann equation expressed as

$$i\hbar \frac{\partial \hat{\rho}}{\partial t} = S^{-1}\hat{H}\hat{\rho} - \hat{\rho}S^{-1}, \tag{3}$$

where $\hat{\rho}$ is the single electron density matrix, $\hat{S}$ is the overlap matrix, and $\hat{H}$ is the system Hamiltonian that includes the external electric field as $\hat{H} = \hat{H}_0 + E_0\delta(t - t_0)\hat{e}$ with $E_0$, the magnitude of the electric field, and $\hat{e}$, its direction. Under the framework of linear response, the adsorbance $I(\omega)$ is calculated as the imaginary part of the Fourier transform of the induced dipole moment caused by an external field. In this study, the external field strength was set to $E_0 = 0.001$ V/Å. The induced dipole moment was evaluated over a 200 fs time period using a time step of $\Delta t = 0.01$ fs. The Fourier transform was performed with an exponential damping function (using a 5 fs damping constant) to eliminate noise.

### C. Quantum–Classical Molecular dynamics

An $\alpha$-alumina surface with a $3 \times 2 \times 1$ supercell is modeled by applying periodic boundary conditions in the x-y direction and a 5 nm vacuum above the surface in the z direction, as shown in Fig. 2a). The optimized alumina surface is equilibrated to 300 K (room temperature) using a Nose-Hoover thermostat. To model the dynamics of molecular adsorption on the alumina surface, different molecules are deposited on a 1 $\text{nm}^2$ target area with a random distribution at the center of the surface using the velocity Verlet algorithm. The time step of 0.25 fs is chosen, and different molecules are emitted at an impact energy of 1 eV, which is chosen respect to the energy bond of the molecules, with 500 independent trajectories, using the same target. Each molecule is emitted vertically with a randomly assigned orientation and an initial distance of 0.6 nm above the surface for a simulation time of 350 fs. The calculations are performed using embarrassing parallelization on 160-240 cores of a computer cluster with a typical wall time of ∼20 min/simulation.

This approach was used in our previous works to investigate the hydrogenation mechanisms of fullerene cages[39] and to study the electronic properties of the 2D nanomaterial borophene, proposed for a boron-based hydrogen detector[40], showing excellent agreement with first principles DFT calculations. SCC-DFTB, as implemented in the publicly available DFTB+ code version 22.1, is used throughout this work for all geometry optimizations and QCMD simulations.

## III. RESULTS AND DISCUSSION

### A. Physisorption pathways

Adsorption calculations were performed on isolated $O_2$, $H_2O$, $CH_4$, and $CO_2$ molecules adsorbed on a {0001} alumina surface. Two cases were considered: an Al–terminated surface, which is non-dipolar, and an oxygen-terminated surface, which is dipolar with half of the oxygen atoms removed from the bottom of the cell. The Al–terminated surface is known to be the most stable of the two, as reported in the literature[41]. During the computations, a 50 Å vacuum section was added above the sample to avoid boundary conditions effects on the calculations and periodic boundary conditions were set in the $x$-$y$ directions to simulate a semi-infinite surface. A $4 \times 4 \times 1$ Monkhorst–Pack set was used for the $k$-point sampling during all calculations. The inter–planar distance of the Al–terminated surface in the bulk is 2.73 Å, while the top layers have a distance of 1.8 Å due to the vacuum section, which reduces the distance by ∼ 45% in agreement with experimental and theoretical data[41,42].

Fig. 2a) shows the adsorbate sites considered in this work for the Al-terminated surface: i) above the top Al atom (labeled Al-1); ii) at the second Al layer with an Al atom and three oxygen atoms as the nearest neighbors (labeled Al-2); iii) the first oxygen layer below the top Al atom, with an oxygen atom next to an Al atom (labeled O-1); and iv) the void between the oxygen atoms at the first O layer (labeled O-2). For the Ox-terminated surface, the optimization process does not affect the geometry of the oxygen atoms layered at the stab top. Here, the Ox–terminated surface is optimized with an oxygen interlayer distance of 2.176 Å between the top layers and 2.187 Å between the layers in the bulk, in fairly good agreement with DFT calculations, reported in the literature[41]. In Fig. 2b), the adsorbate sites for the Ox–terminated surface are presented: i) at the top layer, the place above an oxygen atom defines the O-1 site; ii) the space between the triangle formed by three oxygen atoms is considered the O-2 site; iii) due to the symmetry of the alumina surface, the first Al layer defines the Al-1 site above one Al atom; and iv) the second Al layer is taken into account by defining Al-2 as the vacancy located at the middle of the triangle formed by the top layer's three oxygen atoms and the second layer's six Al atoms. In Fig. 2c), we present the density of states of the supercell sample.

In Fig. 3, we present the energy ($E(z)$) of $O_2$ in a), $H_2O$ in b), $CH_4$ in c), and $CO_2$ in d) molecules at different adsorbate sites on an Al–terminated surface. The orientation of the molecules relative to the surface plane is considered, both parallel and perpendicular. For $O_2$, the minimum contribution is at the adsorbate O–2, where three oxygen atoms repulse the molecule. When oriented perpendicular to the surface, the $O_2$ molecule can be attracted to the Al–1 site and repelled by the Al–2 site. For $H_2O$, the Al–1 and O–1 sites attract the molecule due to the vacancy formed by three oxygen and one Al atoms, and the H atoms are mainly bonded to O atoms from the surface. For $CH_4$, the Al-1 site attracts the molecule due to the interaction of hydrogen atoms with the Al atom, but otherwise, the molecule is mostly repelled by the surface. The results provide insight into the interaction between alumina and these molecules, which is important for understanding chemical processes such as $CO_2$-$CH_4$ reforming and carbon deposition. Finally, for $CO_2$, the molecule is adsorbed by the surface when oriented perpendicularly at the Al-1 and O-2 sites, but the interaction with the C atom and Al is highly repulsive.

The energy ($E(z)$) of $O_2$, $H_2O$, $CH_4$, and $CO_2$ molecules at different adsorbate sites on the Ox–terminated alumina surface is presented in Fig. 4. The oxygen molecule can be attracted to the O–2 adsorbate site, where an Al atom can adsorb the oxygen atom. However, the layer of oxygen atoms can repel the oxygen molecule at distances above 0.5 Å regardless of orientation. The stability of the $O_2$ molecule is observed at distances above 1.5 Å where the Ox–terminated surface has no impact. Under ultra-high vacuum conditions, the clean {0001} surface of alpha-alumina is terminated by a single layer of aluminum atoms. However, in the presence of water, the surface is hydroxylated, making the Ox– terminated surface of interest due to OH bonding. Water molecules are observed to prefer a perpendicular orientation at the O–1 and Al–1 adsorbate sites with the majority of oxygen atoms, as shown in Fig. 4b. The Ox–terminated surface does not interact with the water molecule at distances above 2 Å, while the Al–terminated surface has an interaction range of up to 5.5 Å. The hydrogen atoms of the water molecule tend to interact and bond with the oxygen atoms at Al-1 and O-2 for the perpendicular orientation, but the molecule is mainly repelled by the alumina surface regardless of atom termination. For the Ox–terminated surface, the perpendicularly oriented $CO_2$ molecule is attracted to the site between two O atoms in the surface and the Al atom at the O-1 site, as shown in Fig. 4d. The $CO_2$ molecule is not affected by the Ox–terminated surface for distances above 3 Å, which is larger than the ranges for $O_2$, $H_2O$, and $CH_4$ molecules.

## B. Surface electronic structure

Table I reports the binding energy ($E_b$), length ($z_{\rm min}$), molecular orientation, and adsorbate site to provide more information about the adsorption of molecules by the alumina surface. We also present surface energies, computed as $\gamma_{\rm phys} = E_b/A$, where $A$ is the surface area[41]. This value is a combination of the cohesive energy of surface atoms and the energy required to create a new surface by breaking bonds and is used to determine the sample's equilibrium morphology. The information in the table is used to energy-optimize the alumina surface with different molecules, as shown in Fig. 5 for the Al-terminated surface, which is of interest for experiments. The Ox-terminated surface is found to be less stable than the Al-terminated surface due to the removal of the dipolar nature of the O-terminated plane.

We then performed an optimization process for the Al-terminated surface with different molecules. As expected, the most stable point for the $O_2$ molecule ($O_1$–$O_2$) was above the Al atom (Al-1 site) with an internuclear distance of 0.189 nm to the $O_2$ atom, which decreased by $\sim 3\%$ compared to the isolated molecule, as shown in Fig. 5a. For the $H_2O$ molecule, the distance between the Owater and the Al atom at the top of the surface was 0.317 nm, as shown in Fig. 5b. This location of the $H_2O$ molecules on the Al-terminated surface is related to one of the biggest challenges in the direct reaction between water and aluminum, where the oxide layer on the aluminum surface prevents penetration into the core.

For the $CH_4$ molecule, the bonding between the H atoms and the Al atom of the Al-terminated surface was the minimum compared to the other molecules, as shown in Fig. 5c. The bond length of the H atoms was not affected by physisorption, with an internuclear distance between the most stable adsorbate site (Al-1) and the C atom of 0.250 nm. The physisorption of $CO_2$ by the Al-terminated surface is depicted in Fig. 5d, where $O_{CO2}$ is bound to the Al atom with an internuclear distance of 0.19 nm. The bond length between the C and O atoms was affected by the adsorption of the molecule, explaining the observed dissociation of $CO_2$ in experiments, where adsorbed O atoms produced CO molecules ($CO_2$ = CO + O)[43] with oxygen atoms bound to Al atoms.

The size of the band gap is a crucial parameter in dielectric materials, as it affects thermal carrier tunneling. $\alpha$-Alumina is considered a good dielectric material with a sufficiently large band gap, as demonstrated by the total and partial density of states results shown in Fig. 5. These results are in good agreement with DFT calculations[34]. The adsorption of molecules can greatly alter the density of states (DOS). The pristine alumina peak at +15 eV shifts to +1 eV for all cases due to adsorption, which results in a new gap in the system as determined by the DFTB approach.

The Mulliken charge of an atom is defined as the sum of the orbital populations weighted by their corresponding atomic orbital (AO) coefficients. In this study, the DFTB method is used to compute the Mulliken charge of individual atoms in the system, as seen in Fig. 6a). The histogram of the Mulliken charge of each atoms in the system defined by the Al-terminated surface with each adsorbed molecule at their binding energy distance. It is noted that the oxygen atoms of the alumina surface are highly affected by the adsorption of the molecules, with $CH_4$ having the greatest effect and $CO_2$ having the least effect on the charge distribution of the surface. The adsorption properties of $\alpha$-alumina can be determined using spectroscopic techniques such as UV–visible spectroscopy or infrared spectroscopy. These properties can be utilized in the development of sensors that respond to specific wavelengths of light and to promote chemical reactions when exposed to light. In Fig. 6b, the optical adsorption response of alumina with different molecules on its surface is presented. It is observed that alumina increases its adsorption in the range of 400 to 700 nm, and the presence of $O_2$ and $CH_4$ molecules further enhances its adsorption in the visible range. Results for $H_2O$ with adsorbance spectra is in a qualitatively good agreement with experimental data[19] where the observed peaks are presumably related to the surface instabilities due to the presence of water molecules.

### C. Dynamical molecular adsorption

We compute the probability of reflection and adsorption of $O_2$, $H_2O$, $CH_4$, and $CO_2$ molecule emissions on the Al–terminated alumina surface at 1 eV of kinetic energy to investigate the adsorption and dissociation mechanism dynamically at room temperature, using the approach described in Section 2.3. If the kinetic energy is too low, molecules can be only adsorbed with a low probability of dissociation. The probabilities shown in Fig. 7 are calculated as the $N_{A,R}/N_{\mathrm{Tot}}$ ratio, where $N_{\mathrm{Tot}}$ is the total number of the incident molecules, in our case 500 and $N_{A,R}$ is the number of molecules which are adsorbed or reflected to the surface. Reflected events are determined by measuring a final distance of 1 nm between the Al atoms at the top layer of the surface and the center of mass of the molecules. We notice that $O_2$ molecules are mainly adsorbed by the alumina surface and $CH_4$ molecules are less adsorbed, in good agreement with the physisorption calculations presented in Fig. 3.

In Fig. 8, we present the final positions of adsorption events for different molecular projectiles. For oxygen molecules, we observed a low dissociation probability of 2% as they mainly bond to Al atoms, forming a hexagonal pattern on the surface. In contrast, water molecules have a higher dissociation probability of 40%, with some of them dissociating into OH+H and producing H atoms upon interaction with the surface. Some water molecules are also both adsorbed and dissociated, leading to hydrogen atoms bonding to the oxygen atoms in the second top layer of the alumina surface, and a few oxygen atoms penetrating the surface and finding a final position next to an oxygen atom, thus modifying the chemical and physical properties of the alumina surface. For $CH_4$ molecules, a few C atoms bond to Al atoms, while some H atoms bond to oxygen and aluminum atoms. Dissociation was observed in all cases, with the most likely dissociation channel being $CH_4 \rightarrow CH_2 + H_2$, suggesting that this process could be used for hydrogen production from methane gas, as reported experimentally in the literature[44]. $CO_2$ molecules were observed to dissociate in all cases, with the common dissociation channel being $CO_2 \rightarrow CO + O$, producing multiple O atoms upon interaction with the surface. The adsorbed C and O atoms were found to accumulate around Al atoms, which could be related the adsorption mechanism observed in some experiments[45]. A video showing the visualization of dissociation processes is included in the supplementary material.

## IV. CONCLUDING REMARKS

In this work, we present a study of physisorption pathways for $\alpha-$ alumina and several molecules are computed to describe the binding of the O, C, or H atoms to the Al and O atoms of the surface for prospective studies of chemical reactions and applications in catalysis and sensor technologies. We performed simulations to calculate the binding energies of $\alpha$–alumina with Al atoms layered at the top of the surface named Al–terminated and a second one defined as Ox–terminated by O atoms at the top surface with $O_2$, $H_2O$, $CH_4$, and $CO_2$ by the self–consistent– charge density–functional tight–binding (SCC–DFTB) method. The surfaces are modeled by slabs with thicknesses determined by convergence of the optimized lattice parameters, in good agreement with other experimental and theoretical results. We follow several physisorption pathways considering different molecular orientations where the most stable physisorbed state on the Al–terminated surface is above the Al atom, while the Ox–terminated state is found to be above the oxygen atom; the former is more stable due to the lower physisorption surface energy. DFTB results show that by comparing the binding energies of the adsorption complexes the preferred adsorption sites are de-

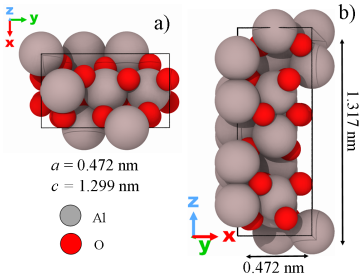

FIG. 1. Structure of an alpha alumina unit cell with 60 atoms (24 Al and 36 O) that was energy optimized by SCC-DFTB.

pendent on the surface structure, Al–terminated and Ox–terminated, as well as the orientation of the molecules, as expected.

Quantum-classical molecular dynamics simulations were performed to investigate the adsorption and dissociation mechanisms. We noted that $O_2$ molecules were mainly adsorbed by the alumina surface, while $CH_4$ molecules were less adsorbed, producing atomic and molecular hydrogen upon interacting with the surface. These molecules also improved the optical adsorption of the alumina surface in the visible range. Based on our calculations, we suggest that the SCC-DFTB approach is suitable for the analysis of dynamical adsorption mechanisms by considering alumina surfaces with an electronic description.

Quantum–Classical Molecular Dynamics simulations are performed to investigate the adsorption and dissociation mechanism. We noted that $O_2$ molecules are mainly adsorbed by the alumina surface, while $CH_4$ molecules are less adsorbed, producing atomic and molecular hydrogen upon interacting with the surface. These molecules also improved the optical adsorption of the alumina surface in the visible range. Based on our calculations, we suggest that the SCC–DFTB approach is suitable for the analysis of dynamical adsorption mechanisms by considering alumina surfaces with an electronic description.

## ACKNOWLEDGEMENTS

We acknowledge support from the European Union Horizon 2020 research and innovation program under grant agreement no. 857470, from the European Regional Development Fund via the Foundation for Polish Science International Research Agenda PLUS program grant No. MAB PLUS/ 2018/8, and INNUMAT project (Grant Agreement No. 101061241). We acknowledge the computational resources provided by the High Performance Cluster at the National Centre for Nuclear Research and the Interdisciplinary Centre for Mathematical and Computational Modelling (ICM) University of Warsaw under computational allocation no g91–1427.

---

[1] J. K. Thomas, *Chemical reviews* **1993**, *93*, 1 301.
[2] B. D. Evans, *Journal of nuclear materials* **1995**, *219* 202.
[3] J.-F. Lin, O. Degtyareva, C. T. Prewitt, P. Dera, N. Sata, E. Gregoryanz, H.-K. Mao, R. J. Hemley, *Nature materials* **2004**, *3*, 6 389.
[4] X. Guo, S. Xu, L. Zhao, W. Lu, F. Zhang, D. G. Evans, X. Duan, *Langmuir* **2009**, *25*, 17 9894.
[5] K. A. Terrani, C. M. Parish, D. Shin, B. A. Pint, *Journal of Nuclear Materials* **2013**, *438*, 1-3 64.
[6] A. Zaborowska, M. Clozel, E. Olivier, J. O'Connell, M. Vanazzi, F. Di Fonzo, A. Azarov, I. Jóźwik, M. Frelek-Kozak, R. Diduszko, et al., *Ceramics International* **2021**, *47*, 24 34740.
[7] S. Blanck, S. Loehle, S. N. Steinmann, C. Michel, *Tribology International* **2020**, *145* 106140.
[8] J. Rey, S. Blanck, P. Clabaut, S. Loehlé, S. N. Steinmann, C. Michel, *The Journal of Physical Chemistry B* **2021**, *125*, 38 10843.
[9] S. Xu, E. A. Carter, *Chemical reviews* **2018**, *119*, 11 6631.
[10] A. Munitz, M. Metzger, R. Mehrabian, *Metallurgical transactions A* **1979**, *10*, 10 1491.
[11] K. M. Shorowordi, T. Laoui, A. A. Haseeb, J.-P. Celis, L. Froyen, *Journal of Materials Processing Technology* **2003**, *142*, 3 738.
[12] W. Huo, S. Wang, X. Zhang, K. Ren, S. Tan, F. Fang, Z. Xie, J. Jiang, *Vacuum* **2022**, *202* 111135.
[13] Y. Su, S. Cui, Z. Zhuo, W. Yang, X. Wang, F. Pan, *ACS Applied Materials & Interfaces* **2015**, *7*, 45 25105.

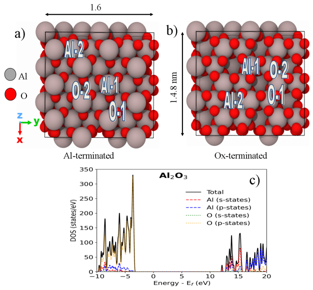

FIG. 2. Alumina surface used to calculate binding energies with identified adsorbate sites considering aluminium and oxygen layers at the top of the surface. Density of states are shown in c).

[14] D. Ferri, T. Bürgi, A. Baiker, *The Journal of Physical Chemistry B* **2001**, *105*, 16 3187.
[15] S. E. Mason, C. R. Iceman, K. S. Tanwar, T. P. Trainor, A. M. Chaka, *The Journal of Physical Chemistry C* **2009**, *113*, 6 2159.
[16] P. Dupiano, D. Stamatis, E. L. Dreizin, *International Journal of Hydrogen Energy* **2011**, *36*, 8 4781.
[17] Y. Tong, J. Wirth, H. Kirsch, M. Wolf, P. Saalfrank, R. K. Campen, *The Journal of Chemical Physics* **2015**, *142*, 5 054704.

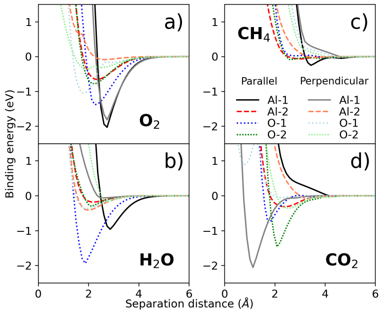

FIG. 3. Physisorption of O$_2$ in a), H$_2$O in b), CH$_4$ in c), and CO$_2$ in d) on the alumina surface for Al–terminated by considering all adsorbate sites. Molecular orientation is included in the calculations

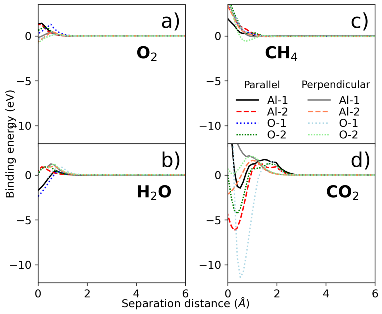

FIG. 4. Binding energy results for physisorption paths for H$_2$O on alumina surface for Al–terminated a) and Ox–terminated in b), considering all the adsorbate sites. Two different orientations are considered in the calculations

TABLE I. Binding energy, $E_b$ [eV] and energy surface $\gamma_{\rm phys}$ [eV/nm$^2$] of alumina surface with different molecules

| Al–terminated | | |
|---|---|---|
| Molecule | $E_b$ | $\gamma_{\rm phys}$ |
| O$_2$ | -2.03 | 0.85 |
| H$_2$O | -1.94 | 0.82 |
| CH$_4$ | -0.25 | 0.11 |
| CO$_2$ | -2.05 | 0.87 |
| **Ox–terminated** | | |
| Molecule | $E_b$ | $\gamma_{\rm phys}$ |
| O$_2$ | -3.03 | 1.28 |
| H$_2$O | -3.14 | 1.33 |
| CH$_4$ | -0.53 | 0.22 |
| CO$_2$ | -11.38 | 4.80 |

[18] D. Qi, K. Kwong, K. Rademacher, M. O. Wolf, J. F. Young, *Nano Letters* **2003**, *3*, 9 1265.

[19] Y. Tong, J. Wirth, H. Kirsch, M. Wolf, P. Saalfrank, R. K. Campen, *The Journal of Chemical Physics* **2015**, *142*, 5 054704.

[20] M. Cabrejas Manchado, J. M. Guil, A. Perez Masia, A. Ruiz Paniego, J. M. Trejo Menayo, *Langmuir* **1994**, *10*, 3 685.

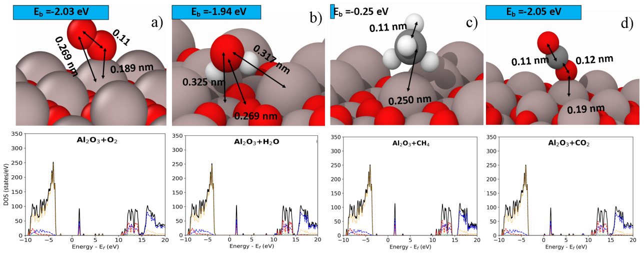

FIG. 5. Most stable adsorption configuration diagram and DOS results for the Al–terminated surface with O$_2$ in a), H$_2$O in b), CH$_4$ in c), and CO$_2$ in d) at the adsorbate site where $E_b$ is minimum. We add a blue bar that represents the magnitude of the binding energy.

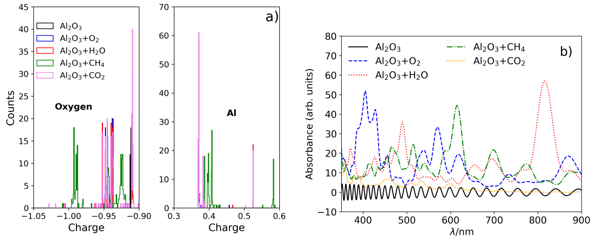

FIG. 6. The Mulliken charge of each atom of different molecules adsorbed by the alumina surface is displayed in a) as a histogram, and Absorbance spectra in b) of alumina with several molecules. CH$_4$ highly affects the charge distribution of the surface

[21] L. Shi, S. Meng, S. Jungsuttiwong, S. Namuangruk, Z.-H. Lu, L. Li, R. Zhang, G. Feng, S. Qing, Z. Gao, X. Yu, *Applied Surface Science* **2020**, *507* 145162.

[22] G. Feng, M. V. Ganduglia-Pirovano, C.-F. Huo, J. Sauer, *The Journal of Physical Chemistry C* **2018**, *122*, 32 18445.

[23] X. Yu, X. Zhang, S. Wang, G. Feng, *Applied Surface Science* **2015**, *343* 33.

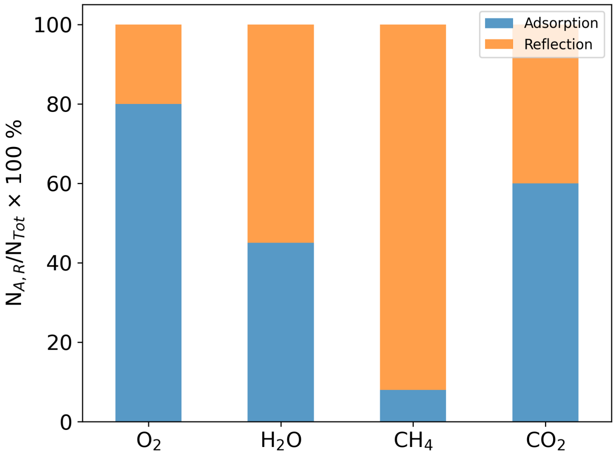

FIG. 7. Reflection and adsorbtion rates for different emitting molecules at 1 eV on alumina surface. Dissociation of molecules are observed during the dynamics.

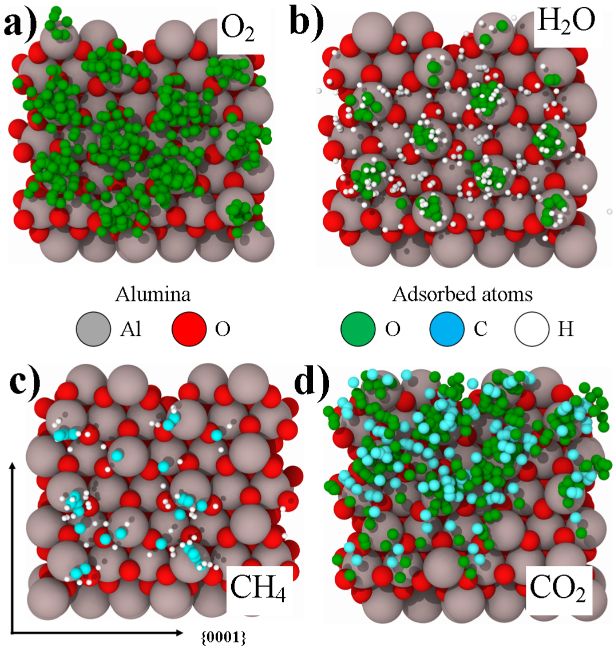

FIG. 8. Final position of all adsorbed atoms after 1 eV emition of 500 molecules of $O_2$ in a), $H_2O$ in b), $CH_4$ in c), and $CO_2$ in d). Atoms and/or molecules are more likely to be bond to an Al at the top layer of the surface. .

[24] S. Hong, A. C. van Duin, *The Journal of Physical Chemistry C* **2015**, *119*, 31 17876.

[25] H.-T. Luu, S. Raumel, F. Dencker, M. Wurz, N. Merkert, *Surface and Coatings Technology* **2022**, *437* 128342.

[26] S. Wang, W. Huo, H. Feng, X. Zhou, F. Fang, Z. Xie, J. K. Shang, J. Jiang, *Small* **2022**, *18*, 40 2203713.

[27] S. Wang, B. Xu, W. Huo, H. Feng, X. Zhou, F. Fang, Z. Xie, J. K. Shang, J. Jiang, *Applied Catalysis B: Environmental* **2022**, *313* 121472.

[28] S. Wang, W. Huo, F. Fang, Z. Xie, J. K. Shang, J. Jiang, *Chemical Engineering Journal* **2022**, *429* 132410.

[29] B. Hourahine, B. Aradi, V. Blum, F. Bonafe, et al., *The Journal of Chemical Physics* **2020**, *152*, 12 124101.

[30] C. KĂ¶hler, G. Seifert, U. Gerstmann, M. Elstner, H. Overhof, T. Frauenheim, *Phys. Chem. Chem. Phys.* **2001**, *3* 5109.

[31] T. A. Niehaus, S. Suhai, F. Della Sala, P. Lugli, M. Elstner, G. Seifert, T. Frauenheim, *Phys. Rev. B* **2001**, *63* 085108.

[32] A. J. Page, Y. Wang, H.-B. Li, S. Irle, K. Morokuma, *The Journal of Physical Chemistry C* **2013**, *117*, 28 14858.

[33] P. Koskinen, V. MĂ¤kinen, *Computational Materials Science* **2009**, *47*, 1 237.

[34] J. Frenzel, A. F. Oliveira, H. A. Duarte, T. Heine, G. Seifert, *Zeitschrift fĂĽr anorganische und allgemeine Chemie* **2005**, *631*, 6-7 1267.

[35] R. Luschtinetz, A. F. Oliveira, J. Frenzel, J.-O. Joswig, G. Seifert, H. A. Duarte, *Surface Science* **2008**, *602*, 7 1347.

[36] L. GuimarĂŁes, A. N. Enyashin, J. Frenzel, T. Heine, H. A. Duarte, G. Seifert, *ACS Nano* **2007**, *1*, 4 362.

[37] D. M. Marquez, C. G. SĂ˘nchez, *Phys. Chem. Chem. Phys.* **2018**, *20* 26280.

[38] M. B. Oviedo, C. F. A. Negre, C. G. SĂ˘nchez, *Phys. Chem. Chem. Phys.* **2010**, *12* 6706.

[39] F. J. Dominguez-Gutierrez, P. S. Krstic, S. Irle, R. Cabrera-Trujillo, *Carbon* **2018**, *134* 189.

[40] M. Novotny, F. J. Dominguez-Gutierrez, P. Krstic, *J. Mater. Chem. C* **2017**, *5* 5426.

[41] N. H. de Leeuw, S. C. Parker, *Journal of the American Ceramic Society* **1999**, *82*, 11 3209.

[42] T. T. Song, M. Yang, J. W. Chai, M. Callsen, et al., *Sci. Rep.* **2016**, *6* 29221.

[43] M. B. Bahari, C. R. Mamat, A. A. Jalil, N. S. Hassan, W. Nabgan, H. D. Setiabudi, D.-V. N. Vo, B. T. Phuong Thuy, *International Journal of Hydrogen Energy* **2022**.

[44] J. Yoo, Y. Bang, S. J. Han, S. Park, J. H. Song, I. K. Song, *Journal of Molecular Catalysis A: Chemical* **2015**, *410* 74.

[45] G. Li, P. Xiao, P. Webley, *Langmuir* **2009**, *25*, 18 10666.